

# The influence of microstructure on the failure behaviour of PEEK

JIA-NI CHU\*, JEROLD M. SCHULTZ

*Materials Science Program and Center for Composite Materials, University of Delaware, Newark, Delaware, USA*

In this study, different molecular weight PEEK materials were used to determine the effect of spherulite size on fracture. Melt processing of the PEEK at different temperatures produced samples of different average spherulite size. A permanganic etching technique was used to reveal the spherulites. It was found that for low molecular weight 150P PEEK, the spherulite size increased with melt processing temperature; but, for the higher molecular weight 450G PEEK, the spherulite size remained approximately constant. Also, the average spherulite size was markedly lower for the material of higher molecular weight. The failure behaviour of these samples was studied using a compact tension test. It was found that the fracture toughness of PEEK varied with processing temperature. Also, the average spherulite size of this material had a profound influence on the fracture mechanism.

## 1. Introduction

Poly(ether-ether-ketone), or PEEK, is currently one of the most studied semicrystalline, thermoplastic materials. The reasons for its popularity stem from its good thermal stability [1], excellent toughness [2], outstanding chemical and solvent resistance, and low flammability [3-5]. It is also used as a matrix material for advanced composite materials.

Recently, it has been shown that the properties of matrix materials have a profound influence on some bulk properties of composite materials [6-11]. The failure behaviour of the semicrystalline matrix material depends on microstructural details such as spherulite size (size of a large, radial aggregate of crystallites which was formed by the polymer chains during solidification), orientation, degree of crystallinity, and degree of transcrystallinity (oriented crystallization at a free fibre-polymer interface). For PEEK and other materials, characterization of these structural features is the starting point for materials research. This present work deals principally with the effects of spherulites on fracture toughness and mechanisms in PEEK.

It has been well established that thermal history and molecular weight are two major factors affecting the spherulite size of a semicrystalline thermoplastic material [11-17]. The final spherulite size depends on nucleation density (number of nuclei per unit volume), as well as the time and temperature used to achieve completely volume-filling spherulites. Nucleation density is commonly altered due to the large temperature range in which crystals melt in semicrystalline polymeric materials. During melt processing, any unmelted crystals can act as a nucleation site for the crystallization of the polymer [17]. Furthermore, the higher the melt processing temperature, the lower the

likelihood that any crystals will survive. Similar concerns are present for the melt time. In this way, if the crystallization time is long enough, the final spherulite size depends upon the melting temperature through the nucleation density.

Once a sample of established spherulite size is obtained, its failure behaviour can be determined and may be a function of the spherulite size [18, 19]. Failure has been shown to proceed by interchain slippage, fracture between crystals, or fracture through or between spherulites [20-22]. To date, the conditions under which each fracture mechanism dominates have not been quantitatively defined.

The objective of this work is to study the morphology (using scanning electron microscopy, [SEM]), fracture toughness and fracture mechanisms (using compact tension test) of "Vitrex 1" 150P (molecular weight  $\approx 23000$ ) and 450G (molecular weight  $\approx 50000$ ) PEEK [23]. To control and develop different spherulite sizes, the PEEK was melt-processed at different temperatures and crystallization was performed under quiescent conditions.

## 2. Experimental details

All specimens were made by compression moulding. Specimens were first melted at 360°C for 30 min and then held at 380, 400 or 420°C for 1 h. All specimens were subsequently quenched to an isothermal crystallization temperature of 310°C where they were held for 4 h to allow them sufficient time to become completely spherulitic. It should be mentioned that oxidation, voids, and uneven temperature distributions are all concerns which may have various effects on the final polymer sample. The effects of these concerns should be represented in the final sample micro-

\* Present address: Fibrous Materials Research Center and Department of Materials Engineering, Drexel University, Philadelphia, Pennsylvania, USA.

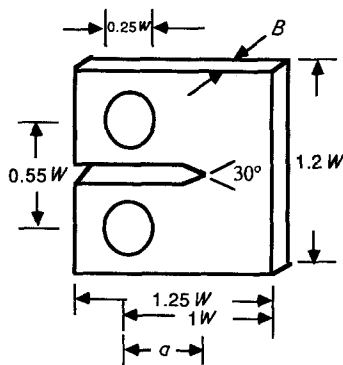


Figure 1 Compact tension test specimen.  $W = 2.54$  cm (1 in),  $a = 1.27$  cm (0.5 in),  $B = 0.32$  cm ( $\frac{1}{8}$  in) for melting temperature 380 and 420° C,  $B = 0.51$  cm, 0.38 cm 0.32 cm, 0.25 cm ( $\frac{1}{5}$  in,  $\frac{3}{20}$  in,  $\frac{1}{8}$  in,  $\frac{1}{10}$  in) for melting temperature 400° C specimens.

structure, and in this way they have not been neglected [24].

The spherulite size of PEEK was determined by polishing the surface of the specimen, and, using a permanganic etching technique [25], subsequent visualization using SEM. A compact tension test [26] was used to measure the fracture toughness of PEEK. Fig. 1 shows the dimensions of the specimen used in the test. To conduct the compact tension test, the specimen was loaded at a constant strain rate in an Instron servohydraulic mechanical testing unit (Model 1125) under uniaxial tension. An extensometer was calibrated and inserted into a machined notch in the sample. A cross-head speed of  $0.127$  cm  $\text{min}^{-1}$  ( $0.05$  in  $\text{min}^{-1}$ ) was used. All tests were performed at room temperature. From these experiments, load against crack-opening displacement data were obtained. The stress intensity factor  $K_{IC}$  (i.e. fracture toughness) of the samples was determined using the following relation [26]

$$K_{IC} = (P/Bw^{1/2}) [29.6(a/w)^{1/2} - 185.5(a/w)^{3/2} + 655.7(a/w)^{5/2} - 1017(a/w)^{7/2} + 639(a/w)^{9/2}]$$

where  $P$  is the load,  $B$  is the thickness of the sample,  $w = 2.54$  cm (1 in) and  $a = 1.27$  cm ( $\frac{1}{2}$  in) in this experiment. After the compact tension test, the specimen was gold-sputtered and examined by SEM in order to reveal the role of spherulites on fracture.

### 3. Spherulite size characterization

On the average, spherulites are radially symmetric polycrystalline arrays, formed when polymers are crystallized from the bulk. Their growth initiates from a nucleus. The nucleus can be an impurity or a crystallite of the original polymer. Once nucleated, lamellae grow radially from the centre [27, 28]. The permanganic etching and morphological study of spherulite sizes in 150P PEEK showed that different melting temperatures resulted in obvious spherulite size differences. Fig. 2 shows an SEM micrograph of a typical spherulite size distribution of etched 150P PEEK melted at 420° C. It was found that for 150P PEEK, the nucleation density decreased as expected with increasing melting temperature. The spherulite size is characterized here

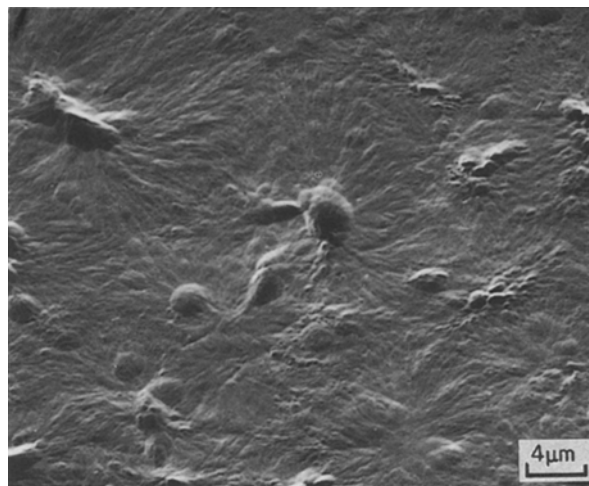


Figure 2 SEM micrograph of spherulites in 150P PEEK (melt processed at 420° C).

by the average size of the five largest observed spherulites: 8.5, 12.7, and 15.3  $\mu\text{m}$  in the 380, 400, and 420° C melt-processed PEEK specimens, respectively. Thus, after volume-filling crystallization, larger spherulites were found in the samples with higher melting temperatures. Clearly, the spherulite nucleation density decreases with increasing melt temperature. This effect may be due to increased dissolution of remnant crystallinity, or to polymer degradation. These effects have been discussed by Kumar *et al.* [29], who made PEEK specimens at temperatures similar to those used in this study. However, due to the well protected melt-processing procedure [24], lack of colour change in the final specimen, and the removal of the most easily oxidized part of the specimen surface, it is unlikely that significant degradation was detected.

In 450G PEEK, the relative loose, long, and easily etched lamellar spherulitic structures of 150P PEEK were no longer observed. SEM micrographs of etched surfaces of 450G PEEK (Fig. 3) showed densely packed, sheaflike (or nascent) spherulites composed of very short lamellae. Fig. 4 is a schematic of the sheaflike microstructure. This microstructure has been

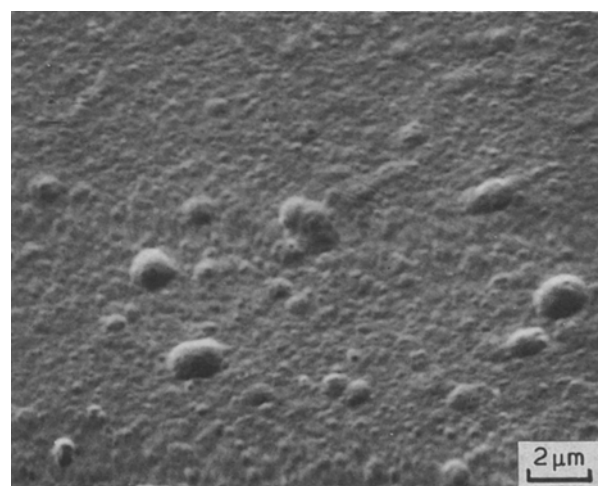


Figure 3 SEM micrograph of spherulites in 450G PEEK (melt processed at 380° C).



Figure 4 A schematic of the sheaflike structure in 450G PEEK.

reported previously for PEEK [29–31]. The sheaflike structure is due ultimately to the high molecular weight of 450G PEEK. According to a theory proposed by Bassett [32], nucleation is strongly affected by molecular weight. Higher molecular weight leads to higher nucleation densities. Thus, using a material with a different molecular weight, or perhaps degrading a given material to a different molecular weight might effect spherulite size.

The small size of the nascent spherulites in the 450G PEEK can be explained based upon a very high nucleation density, which caused the outward growth of a spherulite to cease when it had impinged upon the growing surfaces of adjacent spherulites [33, 34]. The growth of the spherulites in the high nucleation density 450G PEEK was stopped by other spherulites before they had developed the long lamellae bundles characteristic of 150P PEEK. The approximately  $2\ \mu\text{m}$  spherulites observed in these samples were assumed to be restricted to the characteristic size of a nucleus. However, the accurate measurement of size for these sheaflike entities was limited by the resolution of the SEM used. It is believed that if one were to use a higher resolution microscope (e.g. transmission electron microscope), then the actual size of the spherulites would follow the same trend as observed for 150P PEEK — i.e., the samples processed at the highest temperature would give the largest spherulites. Support for this assumption lies in the micrographs of the initial crack surface of 450G samples. This will be discussed in the next section.

#### 4. Fracture toughness and mechanism

The effect of melting temperature on fracture toughness is shown in Fig. 5. Each data point was generated from at least three different specimens. The error ranges from 0.5 to 7.8%. This error represents uncommonly good reproducibility for polymer fracture studies. The above figure shows that for 150P PEEK, the fracture toughness decreases with melting temperature. Since spherulite size increases with increasing melt temperature, it follows that the fracture toughness decreases with spherulite size. These trends are common for other materials, and have been observed by other researchers with materials of different spherulite size [19–21]. For 450G PEEK, although the spherulite size of the sample appeared to be constant (as mentioned when discussing spherulite size characterization), the fracture toughness still decreased with melting temperature. An explanation for this based

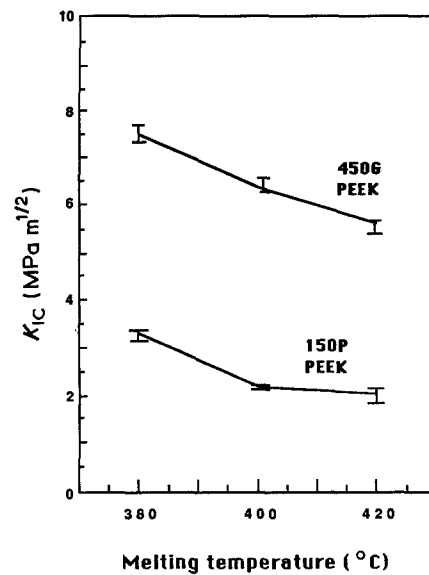


Figure 5 Effect of melting temperature on fracture toughness (sample thickness, 0.32 cm or 1/8 in).

upon small variations in spherulite size still seems reasonable. This is discussed in the following sections which refer to the fracture mechanism of 150P and 450G PEEK.

#### 4.1. 150P PEEK

An SEM analysis of the initial crack surface was performed on fractured 150P PEEK specimens. Fig. 6 is a typical SEM fractograph of a specimen processed at  $380^\circ\text{C}$ . The micrograph shows a common observation for these samples, which will be called “nucleus pull-out”. It is suggested that the knobby apexes of these pyramidal structures consist of a hard nucleus. Attached to these nuclei are lamellae bundles, which are shown in Fig. 6 as the long narrow features connecting the nucleus to the base plane. The very loose arrangement of nuclei and lamellae bundles in the fractured samples seem to reveal features from different depths below the fracture surface.

Figs 7 and 8 are the initial crack surface micrographs for 150P PEEK which had been melt-processed at 400 and  $420^\circ\text{C}$ , respectively. The surfaces show decreasing amounts of nuclei or apexes. Also, even though there is a more open structure around the

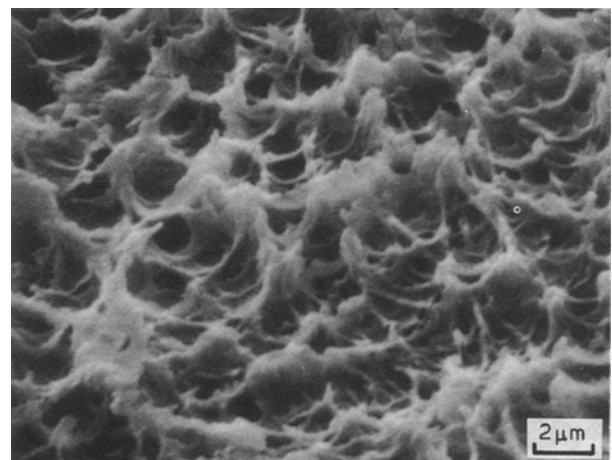


Figure 6 SEM micrograph of initial crack surface in 150P PEEK (melt processed at  $380^\circ\text{C}$ ). Picture shows nucleus pull-out.

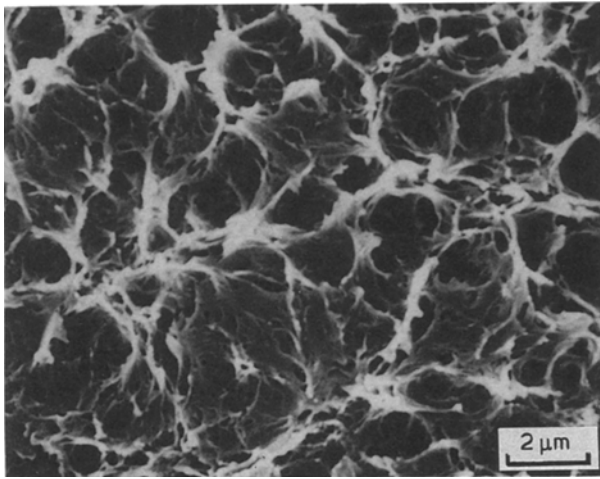


Figure 7 SEM micrograph of initial crack surface in 150P PEEK (melt processed at 400°C). Picture shows relatively fewer nuclei.

nuclei, fewer features seem to be revealed from different depths within the sample. Thus, higher temperatures indicated less nucleus pull-out.

The above features imply that the crack propagated through the spherulite interior. In this way, nuclei were pulled away from the surface by the applied force. Work by others [19–21] has also shown that intraspherulitic cracking can occur in spherulitic materials. Qualitatively, these microstructural features can be related back to fracture toughness through the toughness of the spherulites' constituent components. At higher melting temperatures, 150P specimens show larger spherulites, which are assumed to exhibit smaller (compared to smaller spherulites) density gradients. This density gradient is perceived to run from the high density, high crystallinity nucleus to the low density, low crystallinity boundary. Thus a crack propagates more easily through these types of specimens. In addition, the micrographs (Figs 6, 7, and 8) show circular, drawn structures. The dimension of these structures, associated with the sites where the lamellae attached to the sample, are very similar to those obtained for the originally characterized spherulite size for each specimen. The dimension of these fracture structures increased with increasing processing temperature. Furthermore, the amount of subsurface

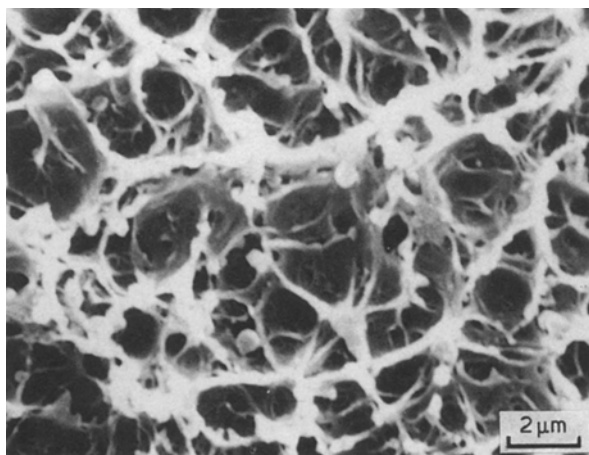


Figure 8 SEM micrograph of initial crack surface in 150P PEEK (melt processed at 420°C). Picture shows relatively fewer nuclei.

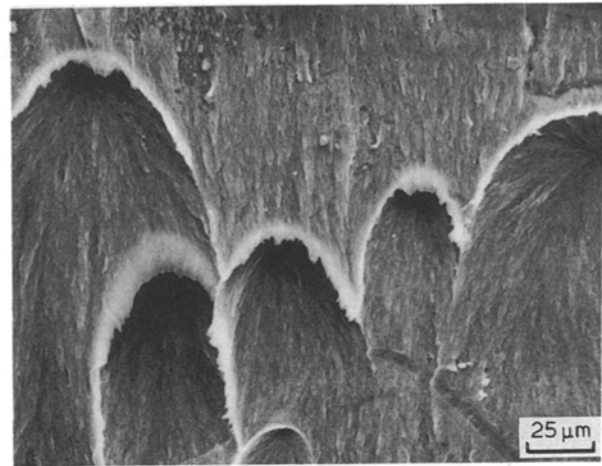


Figure 9 SEM micrograph of initial crack surface in 450G PEEK (melt processed at 420°C). Picture shows all clear features of parabolic curves.

structure appeared to decrease at higher temperatures. This is perhaps a result of the lower nucleation density.

#### 4.2. 450G PEEK

Parabolic fracture surface features, such as seen in Fig. 9, can be found on the fracture surface of polystyrene [35], polymethylmethacrylate [36], polypropylene [36], polyethylene terephthalate (PET) [37], 450G PEEK [38, 39], as well as 450G PEEK fatigue samples [40]. Some investigators, commenting on this kind of structure, have indicated that these features were not dependent on the inner structure of the material [35]. One established explanation for this structure deals with inclusion microcracking. For example, as a crack propagates during mechanical testing, there is also microcracking at some weak points in the region of high stress concentration near the initial crack region. Fig. 10 shows clearly that the centre of this parabolic feature is associated with an inclusion or void. Fig. 11 represents a schematic of the above crack process. As soon as the major crack and a defect-induced microcrack meet, the parabolic curve is formed. After this, the microcrack becomes part of the major crack

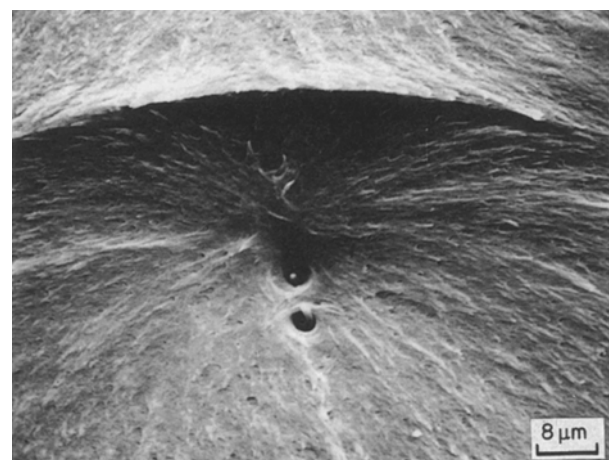


Figure 10 SEM micrograph of fracture surface in 450G PEEK (melt processed at 400°C). The picture shows the impurities or voids at the source of microcrack.

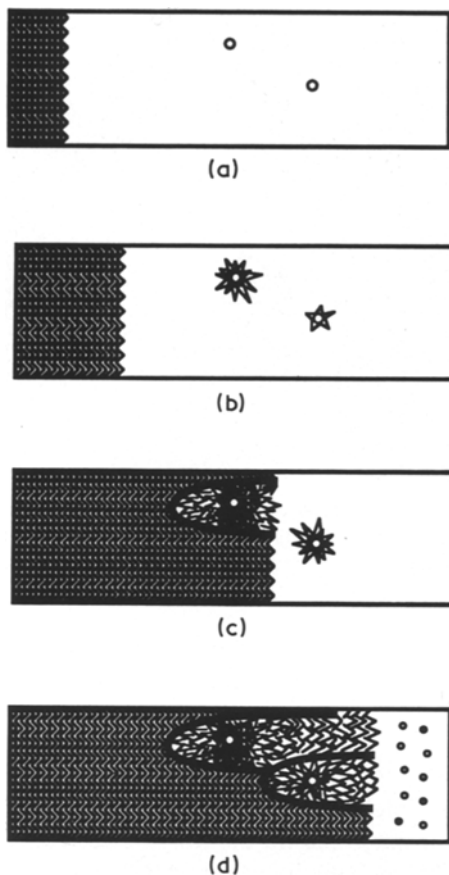


Figure 11 A schematic of the formation of low magnification parabolic curves in 450G PEEK initial crack surface. (a) Major initial crack starts, inclusions exist in the sample. (b) Major crack propagates and microcracks form at inclusions. (c) Parabolic curves are created at initial and microcrack intersection. (d) The initial crack region ends at the crack instability region.

and the cycle continues until another microcrack is encountered. This cycle will end in a crack instability region.

Clearly, impurities or voids cannot be eliminated completely and this phenomenon might be expected in all samples. However, this was not the case. This is thought to be because the term “weak point” represents a relative quantity which depends upon the applied stress. Therefore, only in samples with relatively (relative to the weak points) high stress concen-

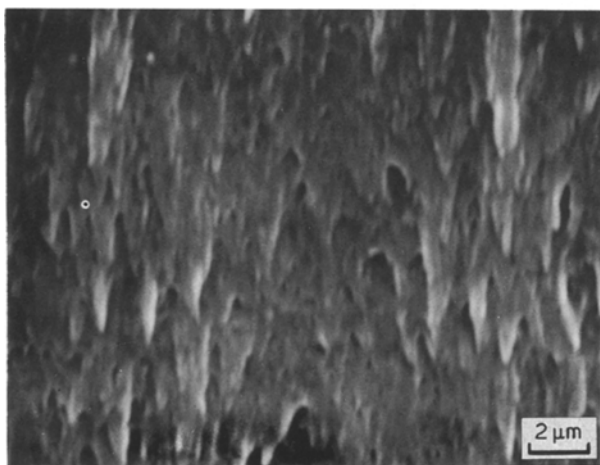


Figure 12 SEM micrograph of initial crack surface in 450G PEEK (melt processed at 380°C). Picture shows the drawn, fingerlike features.

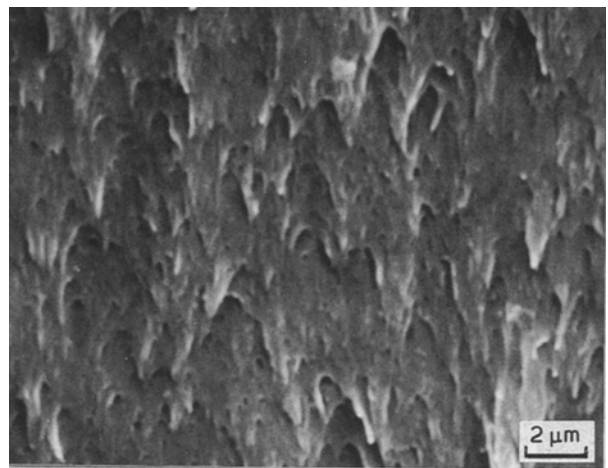


Figure 13 SEM micrograph of initial crack surface in 450G PEEK (melt processed at 400°C). Picture shows the coarse, drawn, fingerlike features.

tration areas (e.g., 450G PEEK) was this phenomenon observed.

As was mentioned earlier for 450G PEEK, there were no significant spherulite size differences, within the limit of resolution of this work, for specimens of different melting temperatures. However, the fracture toughness still showed the same temperature dependence trend as was found for 150P PEEK. This indicates that some microstructure feature or features still played an important role in fracture. The high magnification micrographs of the initial crack surface of 450G PEEK (Figs 12, 13, and 14) show drawn, fingerlike features. These features may be related to the underlying spherulites and differences in spherulite size [41]. Assuming that 450G PEEK is composed of nascent spherulites with a predominantly hard nucleus and very short lamellae bundles (as was shown in Fig. 4), it is very unlikely that the crack would propagate through these hard structures. Thus, an interspherulitic cracking mechanism is proposed for these samples containing very small and hard spherulites. Fig. 15 is a schematic representation of the fracture surface. The fracture is assumed to have followed a path between sheaflike spherulites because this region

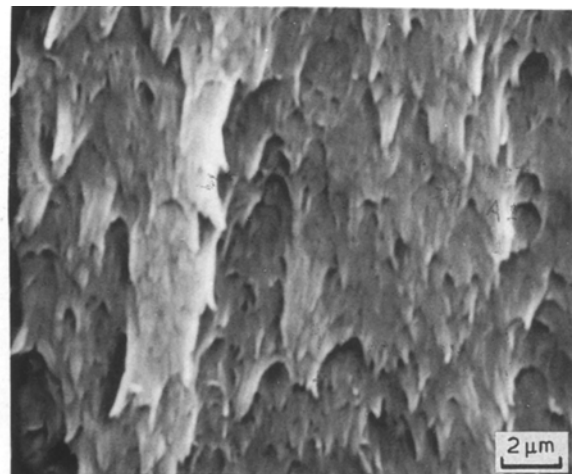


Figure 14 SEM micrograph of initial crack surface in 450G PEEK (melt processed at 420°C). Picture shows that the coarseness of the drawn, fingerlike structure increases with processing temperatures.

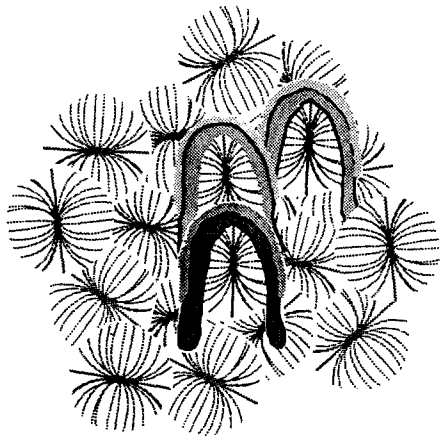


Figure 15 A schematic of plastic hood shape on the fracture surface of 450G PEEK.

has relatively low crystallinity and is the weakest part of the material. Therefore, the nascent spherulites, shown as the light lines in Fig. 15 are actually covered by this lower crystalline and deformed material. The stresses are thought to deform this low crystallinity material around the spherulites, forming the finger-like, plastic hood shapes. This is shown by the dark lines in Fig. 15. These features were the ones seen in the SEM micrographs of the actual fracture surfaces (Figs 12, 13, and 14).

If the above is realized, then the size of the fingerlike structure should be directly related to the size of the underlying nascent spherulite and to the amount of amorphous material between the spherulites. Furthermore, as the crack propagates, it should go around these spherulites which have relatively high density gradients. These circuitous paths would add depth to the fracture surface. Thus, large spherulites should display a rougher fracture surface. This was found in Fig. 14.

The general contention throughout this work has been that higher melting temperatures lead to larger spherulite sizes or lower spherulitic densities. For the case of 450G PEEK, more work needs to be done to test the hypothesis stated above.

## 5. Conclusions

Based upon the findings in this study for different molecular weight PEEK, the following conclusions were obtained:

(1) For lower molecular weight 150P PEEK materials, spherulite size increased dramatically with melting temperature, following a crystallization treatment of fixed crystallization temperature and time. However, for the higher molecular weight 450G PEEK materials, because of high nucleation density, spherulite size differences became too small to be observed under SEM.

(2) Characteristics of spherulite size are reflected in the morphology of the fracture surface. Observations of these morphologies for 450G PEEK indicated that the variation of spherulite size with melting temperature followed the same trend as observed in 150P PEEK — i.e. higher temperatures yielded larger spherulites.

(3) The spherulite size of PEEK was greatly influenced by the molecular weight, the higher molecular weight polymer having the smaller spherulite dimensions.

(4) In PEEK specimens, the fracture toughness data obtained by a compact tension test indicated that the fracture toughness decreased with increasing melting temperature.

(5) The fracture surface study of 150P PEEK indicated that intraspherulitic fracture occurs in this material. A common morphological feature in these samples is termed nucleus pull-out.

(6) The fracture surface study of 450G PEEK indicated that interspherulitic fracture occurred in this material. A common morphological feature in these samples is a drawn, fingerlike structure.

(7) Low magnification SEM micrographs showed parabolic structures in the initial crack surface of 450G PEEK. The parabolic features were initiated by microcracking at relatively high stress concentrations near voids or inclusions; thus, these features are not related to the intrinsic microstructure of the material.

## Acknowledgement

This work was supported by US Army Research Office under grant DAAG29-85-K-0042.

## References

1. D. J. BLUNDELL and B. N. OSBORN, *Polymer* **24** (1983) 953.
2. O. B. SEARLE and R. H. PFEIFFER, *Polym. Eng. Sci.* **25** (1985) 474.
3. D. W. CLEGG and A. A. COLLYER, "The Mechanical Properties of Reinforced Thermoplastics" (Elsevier Applied Science Publishers, New York, 1984).
4. G. R. BELBIN, Proceedings of the 12th John Player Lecture, London, 1984.
5. D. J. KEMMISH and J. N. HAY, *Polymer* **26** (1985) 905.
6. E. J. STOBER, J. C. SEFERIS and J. D. KEENAN, *ibid.* **25** (1984) 1845.
7. J. DELMONTE, "Technology of Carbon and Graphite Fiber Composites", (Von Nostrand Reinhold, New York, 1981).
8. J. C. SEFERIS, A. E. ELIA and A. R. WEDGEWOOD, Proceedings of European Meeting on Polymer Processing and Properties, (Plenum Press, New York, 1984) 423.
9. J. C. SEFERIS, *Polym. Compos.* **7** (1986) 158.
10. C. N. VELISARIS and J. C. SEFERIS, *Polym. Eng. Sci.* **26** (1986) 1574.
11. W. J. SICHINA and P. S. GILL, *ANTEC* (1985) 293.
12. C. H. MICHLER and I. NAUMANN, Proceedings 17th Europhysics Conference on Macromolecular Physics (Walter de Gruyter, New York, 1986) p. 329.
13. J. H. REINSHAGEN and R. W. DUNLAP, *J. Appl. Polym. Sci.* **17** (1973) 3619.
14. J. R. COLLIER and L. M. NEAL, *Polym. Eng. Sci.* **9** (1969) 182.
15. L. B. MORGAN, *J. Appl. Chem.* **4** (1954) 160.
16. J. V. McLAREN, *Polymer* **4** (1963) 175.
17. B. WUNDERLICH, "Macromolecular Physics" (Academic, New York, 1976).
18. L. W. KLEINER, M. R. RADLOFF, J. M. SCHULTZ and T. W. CHOU, *J. Polym. Sci., Polym. Phys. Edn.* **12** (1974) 819.
19. J. L. WAY, J. R. ATKINSON and J. NUTTING, *J. Mater. Sci.* **9** (1974) 293.
20. K. FRIEDRICH, *Fracture* **3** (1977) 1119.
21. J. M. SCHULTZ, *Polym. Eng. Sci.* **24** (1984) 770.

22. R. A. CRICK, D. C. LEACH, P. J. MEAKIN and D. R. MOORE, *J. Mater. Sci.* **22** (1987) 2094.
23. J. DERAUX, D. DELIMOY, D. DAOUST, R. LEGRAS, J. P. MERCIER, C. STRAZIELLE and E. NIELD, *Polymer* **26** (1985) 1994.
24. JIA-NI CHU, M. S. Thesis, University of Delaware (1988).
25. R. H. OLLEY, D. C. BASSETT and D. J. BLUNDELL, *Polymer* **27** (1986) 344.
26. D. BROEK, "Elementary Engineering Fracture Mechanics"; 4th Rev. Edn (Martinus Nijhoff, Dordrecht, Netherlands, 1986).
27. P. H. GEIL, "Polymer Single Crystals" (Interscience, New York, 1963).
28. W. Y. YEH and S. L. LAMBERT, *Macromol. Sci. Phys.* **B6** (1972) 599.
29. S. KUMAR, D. P. ANDERSON and W. W. ADAMS, *Polymer* **27** (1986) 329.
30. A. J. WADDON, M. J. HILL, A. KELLER and D. J. BLUNDELL, *J. Mater. Sci.* **22** (1985) 1773.
31. HEIKE MOTZ, PhD Thesis, University of Delaware (1988).
32. D. C. BASSETT, "Principles of Polymer Morphology" (Cambridge University Press, Cambridge, 1981).
33. J. M. SCHULTZ, "Polymer Materials Science" (Prentice-Hall, New Jersey, 1974).
34. J. M. S. HEARLE, "Polymers and Their Properties, Vol. 1, Fundamentals of Structure and Mechanics" (Ellis Horwood Publishers, England, 1982).
35. F. LEDNICKY, Proceedings 17th Europhysics Conference on Macromolecular Physics, (Walter de Gruyter, New York, 1986) p. 54.
36. F. LEDNICKY and Z. PELZBAUER, *J. Polym. Sci. Part C* **38** (1972) 375.
37. K. FRIEDRICH, Personal Communication, University of Delaware (1988).
38. J. KARGER-KOCSIS and K. FRIEDRICH, *Polymer* **27** (1986) 1753.
39. *Idem.*, *Plast. Rubber Proc.* **8** (1987) 91.
40. K. FRIEDRICH, R. WALTER, H. VOSS and J. KARGER-KOCSIS, *Composites* **17** (1986) 205.
41. W. S. DUBNER, Personal Communication, University of Delaware (1988).

*Received 27 September 1988  
and accepted 13 February 1989*